Desalination and Water Treatment
www.deswater.com

1944-3994/1944-3986 © 2010 Desalination Publications. All rights reserved
doi: 10/5004/dwt.2010.1741

22 (2010) 204–210
October

Enhanced photocatalytic degradation of C.I. Reactive Orange 86 in aqueous environment using nanostructure $Zn_{1-x}Co_xO$ composite thin film coated on glass

Mohammad Hossein Habibi*, Iman Asadi Farsani

Catalysis Division, Department of Chemistry, University of Isfahan, Isfahan, 81746-73441 I.R. Iran
Tel. +98-311-7932707; email: habibi@chem.ui.ac.ir

Received 30 December 2009; Accepted 11 April 2010

ABSTRACT

Nanostructure composite zinc and cobalt oxide thin film coated on flat glass with different Co contents were prepared and characterized by X-ray power diffraction (XRD), UV–vis, atomic force microscope (AFM) and scanning electron microscope (SEM). The results revealed that the particle size of 32 nm and 40 nm for $Zn_{1-x}Co_xO$ and pure ZnO respectively, which is critical for enhancing the photocatalytic activity. The photocatalytic activity of $Zn_{1-x}Co_xO$ was enhanced compared with pure nanostructure zinc oxide thin film. The effects of the cobalt content of $Zn_{1-x}Co_xO$ thin film and dye concentration in the photocatalytic degradation of C.I. Reactive orange 86 were studied. Among the catalysts studied, the $Zn_{0.9}Co_{0.1}O$ thin film was the most active, and the degradation rate of C.I. Reactive Orange 86 (RO) reached maximum when the concentration of the catalyst was 10 mg/l. Final products were, in all cases, CO_2, NH_4^+ and NO_3^- ions and SO_4^{2-} ions.

Keywords: Photocatalytic degradation; $Zn_{1-x}Co_xO$ thin film; Composite thin film; Nanoparticle; Reactive Orange 86

1. Introduction

Wastewater contaminated textile dyes are not readily biodegradable. Conventional methods such as chemical oxidation and activated carbon adsorption suffer from drawbacks, including high cost. Biodegradation is a cost-effective method and environmental friendly, but it is time consuming [1]. Advanced oxidation processes (AOPs) are attractive alternatives to conventional water treatment processes. Among the AOPs, semiconductors as photocatalyst with UV light can be used for degradation of a wide range of organic pollutants [2–10]. Recently, attention has been devoted to the preparation of semiconductors which are promising candidates for applications in photocatalytic oxidation because of their high surface areas [11–18]. Metal oxides, such as ZnO are promising photocatalysts for the oxidation of organic pollutants in aqueous environments. Zinc oxide has been shown to be more efficient in the photocatalytic oxidation of organic pollutants under UV illumination. Pure metal oxides have disadvantages of low quantum yield and the fast recombination rate of photogenerated electron–hole pair. There has been a lot of interest in enhancing the photocatalytic activity of semiconductors for the degradation. The rate of recombination of electron–hole pairs can be easily tuned by modification methods such as selective metal ion doping surface [19–23]. The presence of metals on semiconducting metal oxides which act as electron–hole separation centers can enhance the degradation efficiency of photocatalytic reactions [24]. The electron transfer from the semiconductor conduction band to heavy metal

---

*Corresponding author.

particles at the interface is thermodynamically possible because the Fermi level of semiconductor is higher than that of heavy metal which improves the charge separation and thus enhances the photocatalytic activity of semiconductor [25,26]. The biggest advantage of ZnO is that it can absorb over a larger fraction of UV spectrum and the corresponding threshold of ZnO is 425 nm. Reports on photocatalytic decolorization of methylene blue over $Zn_{1-x}Co_xO$ powder photocatalyst are available [27].

The finely divided powder photocatalyst can be dispersed in the irradiated aqueous solution as slurry [28–29]. However, from a practical point of view it may not be possible to use catalyst suspension in slurry because of the filtration problems linked to the small size of the photocatalyst particles for catalyst recycling and obtaining clean, powder-free water. Because of this reason, attempts have been made to immobilize the catalyst on rigid supports. It has been shown that it is possible to deposit photocatalyst on various rigid supports of different nature such as glass and stainless steel [30–31]. Recently, it was reported that zinc oxide thin film coated on glass bead could degrade azo dyes but the degradation rate was low [32]. To the best of our knowledge there has been no report on the preparation of nanostructure composite $Zn_{1-x}Co_xO$ thin film on glass substrate and their photocatalytic oxidation toward the dye pollutants.

In this work, we have prepared $Zn_{1-x}Co_xO$ thin films via sol–gel dip-coating method, in which Co^{2+} ions were homogeneously incorporated into the lattice of ZnO nanostructure. The properties of $Zn_{1-x}Co_xO$ thin films were studied by X-ray diffraction (XRD), UV-vis spectroscopy (UV-vis) scanning electron microscope (SEM) and atomic force microscope (AFM). C. I. Reactive orange 86 (RO) (chemical structure shown in Fig. 1) degradation was used as a probe reaction to evaluate the role of Co^{2+} substitution in photocatalytic activities of $Zn_{1-x}Co_xO$ thin film in response to UV light irradiation. We have found that Co^{2+} doping markedly enhanced the photodegradation of RO solution under UV light irradiation.

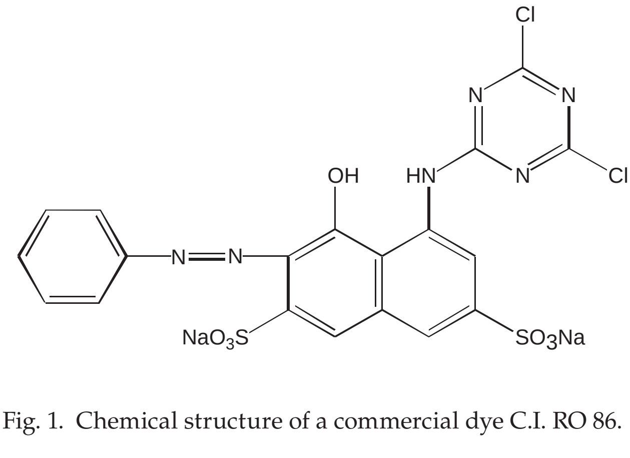

Fig. 1. Chemical structure of a commercial dye C.I. RO 86.

2. Experimental

$Zn_{1-x}Co_xO$ sol was synthesized via an improved sol–gel method. A sample of $Zn(CH_3COO)_2 \cdot 2H_2O$, $Co(CH_3COO)_2 \cdot 4H_2O$, monoethanolamine (MEA) and 1 ml de-ionized water were dissolved in 15 ml isopropyl alcohol at 70°C for 60 min under vigorous stirring. The stoichiometry of cobalt was controlled by dissolving the precursor $Co(CH_3COO)_2 \cdot 4H_2O$ in anhydrous ethanol. The reaction mixture became transparent $Zn_{1-x}Co_xO$ sol and then decanted into a conical bottle. Precursor solution did not produce any precipitation after 50 d. $Zn_{1-x}Co_xO$ thin films were prepared by dip-coating method and dried at 100°C. Films were annealed at 350–550°C for 80 min. The deposition was repeated to obtain a film with different thickness. The structure and crystalline size were determined by XRD diffraction (Bruker D8 advanced X-ray diffractometer: Cu Kα radiation, Scan rate 0.03 2θ s^{-1}). Film morphology was characterized by a C26 DME atomic force microscope (AFM) and Philips XL-30 scanning electron microscopy (SEM) with accelerating 10 kV. Transparency was measured by spectrophotometer (Varian Cary 500 Scan). The BET specific surface area (SSA) was determined for each of the catalysts, using BET apparatus SA 3100 S of Coulter Electronics Inc. The measurements were carried out in the 5-point mode. The initial and final pH values were measured by pH/conductivity-meter, Schott Instruments GmbH, Mainz, Germany. Degradation of dye solutions was monitored by a Double beam UV-visible spectrophotometer (Varian Cary 500 Scan). Total organic carbon content (TOC) measurements was performed by Total Organic Carbon analyzer; Shimadzu TOC-VCPN, Japan. The photocatalytic degradation experiments were carried out in a simple (Fig. 2) oxidation reactor (50 ml), placed in a 25°C water bath. Glass with 5 layers that placed in 25 ml of 5–20 ppm C.I. RO 86 solution was irradiated with two 8W lamps (Philips; $\lambda = 365$ nm) placed 5 cm above the solutions. Concentration is measured by spectrophotometer at λ max of 535 nm (Varian Cary 500 Scan).

In all experiments, 25 ml of RO was used with stirring during the irradiation. Doubly distilled water was used throughout this study and the initial pH of solutions was adjusted as appropriate by addition of either HCl or NaOH. The light intensity was measured by a light intensity meter from Photon Technology International and controlled at 3.0 mW/cm². Solution sample (1 ml/each time) was withdrawn from the fixed film batch reactor for the determination of dye concentration using calibration curve and were poured back into

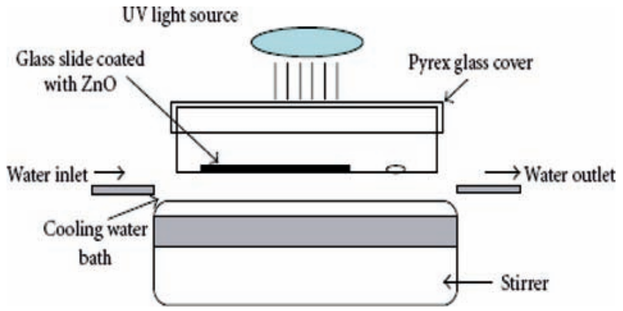

Fig. 2. The diagrammatic representation of the experimental setup used for photocatalytic experiments: glass slide coated with $Zn_{1-x}Co_xO$ thin films, UV light source, pyrex glass cover, reactor and magnetic stirrer.

the reactor after that. The results of blank experiments under similar conditions but without the addition of catalysts indicated that there was a negligible loss of solution volume due to the UV irradiation and reactor open to the air but the loss of substrate was negligible. A comparative study of catalytic activity was performed using $Zn_{1-x}Co_xO$ thin film and pure ZnO thin film. Formation of NH_4^+ and NO_3^- and SO_4^{2-} ions was assayed by high-pressure liquid chromatography (Jasco; CD-5 conductivity detector; Shodex cationic (Y-521) and anionic (I-524) columns). The eluent was a 4 mm HNO_3 solution for the cationic column or a solution of phthalic acid (2.5 mm) and tris (hydroxymethyl) aminomethane (2.3 mm) for the anionic column. Analyses were performed after separation of the photomediator by centrifugation and eventual filtration with an Advantech 0.2 mm PTFE filter. In alkaline media, the NH_3 produced (if any) was detected as NH_4^+ ions on acidification with the HNO_3 eluent during the analyses of cations.

3. Results and discussion

3.1. Catalysts characterization

The BET SSA of $Zn_{1-x}Co_xO$ thin films ranges from 12.23 to 18.25 m^2/g. The highest SSA was determined for $Zn_{0.9}Co_{0.1}O$ thin film while the lowest one was that for $Zn_{0.99}Co_{0.01}O$ thin film.

The UV–vis transmittance spectra of $Zn_{1-x}Co_xO$ thin films with different Cobalt contents is shown in Fig. 3. The band edge for the pure ZnO sample appeared at 3.10 eV (400 nm) while the band edge of the Co doped ZnO thin films shifted to longer wavelengths with increasing cobalt concentration. The red shift of the band gap Eg edge with incorporation of Co into ZnO has been observed and interpreted as mainly due to the sp–d exchange interactions between the band electrons and the localized d electrons of the Co^{2+} ions substituting Zn ions [33–36]. It can be clearly seen that a wider band gap makes photogenerated holes to have a stronger reductive electric potential, which leads to an increase of the photocatalytic efficiency. This could be mainly attributed to the quantum size effect as well as the strong interaction between the surface oxides of Zn and Co. These observations strongly suggest that the Co content significantly affects the particle size and hence influence the absorbance properties.

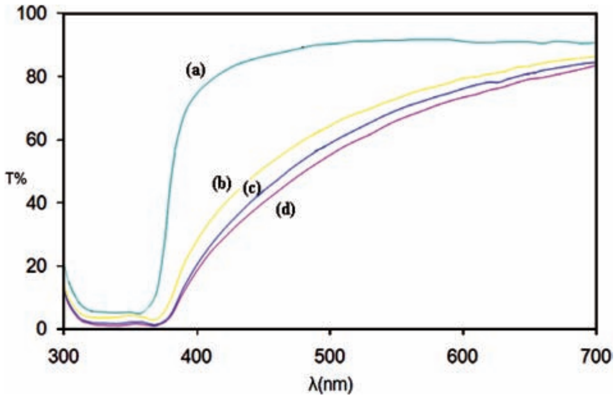

Fig. 3. UV-Visible transmittance spectra of (a) $Zn_{0.99}Co_{0.01}O$ (b) $Zn_{0.97}Co_{0.03}O$ (c) $Zn_{0.95}Co_{0.05}O$ (d) $Zn_{0.9}Co_{0.1}O$ thin films.

The representative XRD patterns of $Zn_{1-x}Co_xO$ thin film is illustrated in Fig. 4. Miller indices of the diffraction peaks are also given. It is shown that the diffraction peaks are relatively strong, and the peak positions matched well the standard data for bulk ZnO. Therefore, all samples crystallized in a wurtzite structure with a high crystallinity [37–42]. The three strongest XRD peaks for ZnO were detected with Miller indices (100), (002) and (101) corresponding to Bragg angles 31.8, 34.5 and 36.4°, respectively. The diffraction peaks were indexed to the hexagonal wurtzite structure (space group P63mc) and the d-values calculated are in good agreement with JCPDS no. 75-1526. The mean crystallite size L was determined from the broadening β of the most intense line, for each polymorph, in the X-ray diffraction pattern, based on the Scherer equation using the full-width at half maximum of the peaks corresponding to the planes (110), (002) and (101):

$$L = \frac{k\lambda}{\beta \cos \theta}$$

where λ is the radiation wavelength, $k = 0.90$ and θ the Bragg angle [43]. The grain size decreases gradually with increasing the time and temperature of calcination up to 500 ^{o}C (smallest grain size of 32 nm). The particle size of $Zn_{1-x}Co_xO$ thin films (32 nm) is smaller than pure

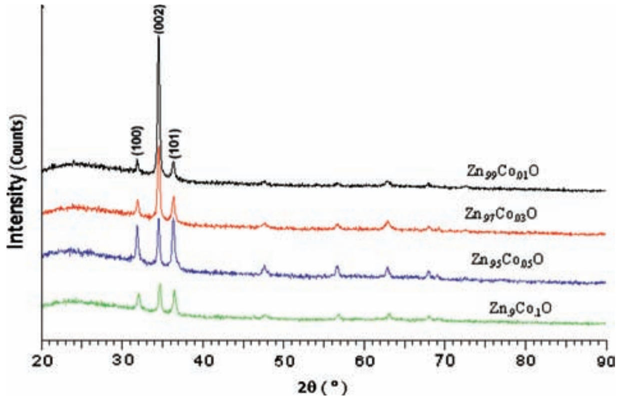

Fig. 4. The XRD pattern of the $Zn_{1-x}Co_xO$ thin film with different cobalt percent coated on glass by dip-coating and annealed at 550 °C.

ZnO (40 nm), attributed to the formation of Co–O–Zn on the surface of the coating [12,32] which hinders the growth of crystal grains. The *X*-Ray diffraction patterns of $Zn_{1-x}Co_xO$ thin films with various molar ratio of cobalt annealed at 550 °C are shown in Fig. 4. A strong (002) preferential orientation has been observed for the pure ZnO thin film which is decreased with increasing amounts of cobalt in $Zn_{1-x}Co_xO$ thin film. As shown in Fig. 4 with increasing of cobalt concentration new peaks appeared which indicates that new mixed zinc cobalt oxide is formed.

The scanning electron microscopy images of $Zn_{1-x}Co_xO$ thin film is shown in Figs. 5(a)–(d). The section of this $Zn_{0.9}Co_{0.1}O$ thin film is also characterized by means of SEM, the testing result shows the average thickness of film is 200 nm. SEM micrographs of the smooth and textures $Zn_{1-x}Co_xO$ l thin films deposited at a growth temperature of 550 °C; (a) and (b) with lower cobalt content, (c) and (d) with higher cobalt content. Figs. 5(a) and (b) presents the SEM images of the nanostructured films of $Zn_{0.99}Co_{0.01}O$ and $Zn_{0.97}Co_{0.03}O$ respectively. As shown in Figs. 5(a) and (b), the film with lower cobalt content is assembled by the spherical nanoparticles that are distributed uniformly and monodispersely in the film. The average crystalline size of $Zn_{1-x}Co_xO$ in the film annealed at 500 °C is about 33 nm and a granular surface. In general, films are homogeneous and continuous. Separate coating layers are not visible in sintered films. Films were crack-free, and had a uniformly distributed grain structure with a thickness of 200 nm [44–46]. Figs. 5(c) and (d) display a SEM images of the nanostructured films with texture surface for $Zn_{0.95}Co_{0.05}O$ and $Zn_{0.90}Co_{0.10}O$ respectively. It is observed from the micrographs that the surface morphology changes as the cobalt concentration increases. The differences on morphologies are noticeable in Figs. 5(a) and (b) rounded grains surfaces for $Zn_{0.99}Co_{0.01}O$ and $Zn_{0.97}Co_{0.03}O$ thin films (lower cobalt content) are observed and there is an

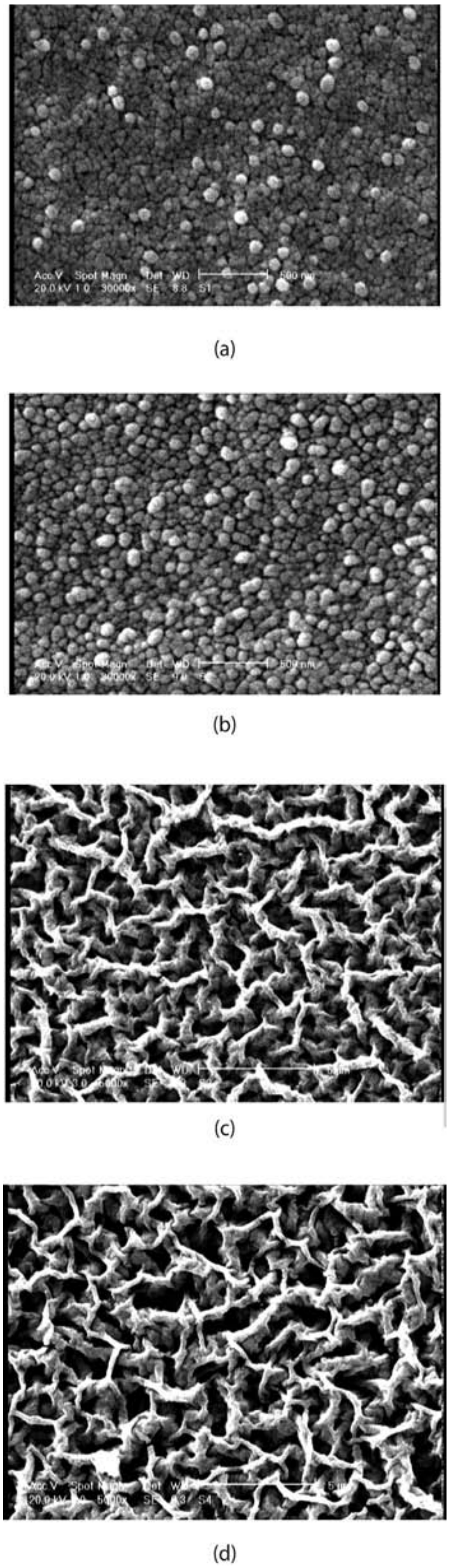
(a)
(b)
(c)
(d)

Fig. 5. SEM image of $Zn_{1-x}Co_xO$ thin film with different cobalt percent coated on glass by dip-coating and annealed at 550 °C (a) $Zn_{0.99}Co_{0.01}O$; (b) $Zn_{0.97}Co_{0.03}O$; (c) $Zn_{0.95}Co_{0.05}O$; and (d) $Zn_{0.9}Co_{0.1}O$.

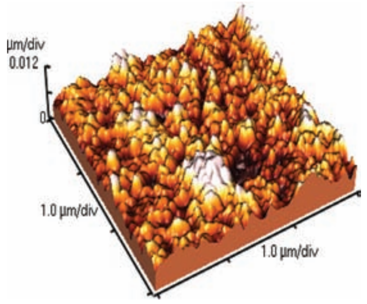

Fig. 6. AFM image of $Zn_{0.9}Co_{0.1}O$ thin film photocatalyst coated on glass.

evolution to texture surface for $Zn_{0.95}Co_{0.05}O$ and $Zn_{0.90}Co_{0.10}O$ films (higher cobalt content) from Fig. 5(c) and (d) [47].

The surface microstructure and morphology at nanometric scale in $Zn_{1-x}Co_xO$ thin films were studied by atomic force microscopy (AFM). As seen from AFM images in Fig. 6, the films are uniform and densely packed. All the films exhibit granular structure. It appears that the incorporation of cobalt atoms significantly affects the microstructure and surface morphology.

3.2 Photodegradation of RO dye by $Zn_{1-x}Co_xO$ thin films

A series of experiments were carried out to measure photocatalytic activity of the $Zn_{1-x}Co_xO$ and ZnO thin films, with RO in aqueous suspension. Fig. 7 shows the effect of $Zn_{1-x}Co_xO$ thin films on photodegradation of RO textile dye compare to pure ZnO thin film (Fig. 8). Photodegradation experiments were carried out at dye concentration 5–20 mg/l, reaction temperature 25°C, catalyst loading 5 glass slide coated with pure ZnO or $Zn_{1-x}Co_xO$ thin films. The self-degradation of RO without involving photocatalysts was negligible under UV light irradiation [48,49]. It is clearly seen from Fig. 7 that the rate of photocatalytic degradation of $Zn_{1-x}Co_xO$ thin film catalysts is higher compared to pure ZnO thin film. It is interesting to note that the rate constant of the catalysts increases with increase in the Co content up to 10 mol % and then decreases. Thus, it is concluded that the optimum loading of Co is 10 mol %, ($Zn_{1-x}Co_xO$) which may be more efficient for separating of photoinduced electron–hole pairs and enhance the photocatalytic activity. Under the irradiation of $Zn_{1-x}Co_xO$ nanostructure thin film cobalt acts as an electron scavenger, which may react with the superoxide species and prevent the holes–electrons recombination, and thus increases photooxidation efficiency [11–15].

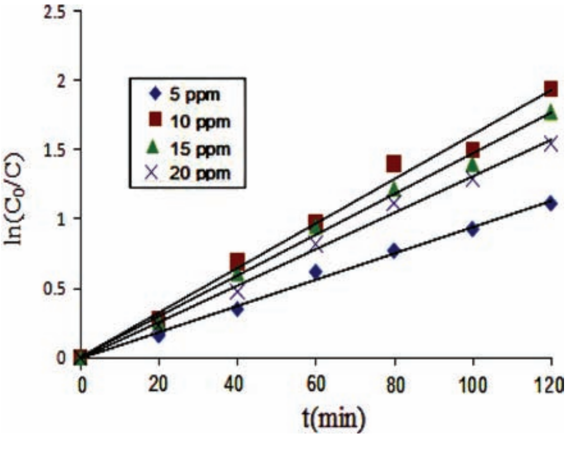

Fig. 7. Effect of UV-irradiation time on the degradation of C.I. RO 86 textile dyes at initial concentrations 5, 10, 15 and 20 mg/l in de-ionized water using $Zn_{1-x}Co_xO$ thin film photocatalyst coated on glass.

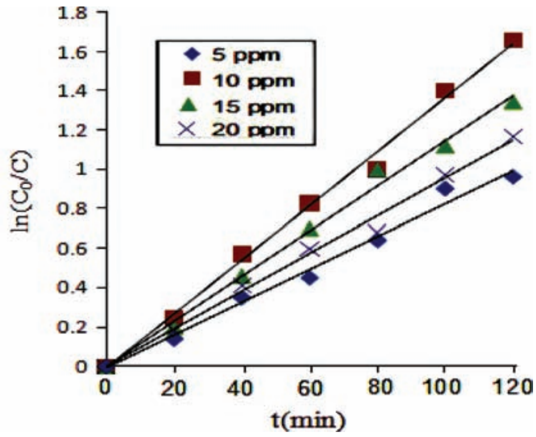

Fig. 8. Effect of UV-irradiation time on the degradation of C.I. RO 86 textile dyes at initial conentration 5, 10, 15 and 20 mg/L in de-ionized water on ZnO thin film photocatalyst coated on glass.

Fig. 7 showed the ln (C_0/C) versus time curves of the RO photocatalytic decolorization using $Zn_{1-x}Co_xO$ photocatalyst, where C_0 and C were the concentrations of the primal and remaining RO, respectively. All curves shown in Fig. 7 were linear, revealing that the kinetic data of the RO photocatalytic decolorization fit well to the first-order reaction kinetic model. Assuming pseudo-first-order reaction kinetics for the photocatalytic oxidation process, the decolorization rate constant was determined from the equation $\ln(C_t/C_0) = -kt$, where C_0 and C_t are the dye concentrations at times 0 and t, respectively, and k is the first-order rate constant [50]. The degradation percent are experimentally determined to be 50.8 for $x = 0.00$, 57.4 for $x = 0.01$, 61.3 for $x = 0.03$, 69.3 for $x = 0.05$ and 78.4 for $x = 0.10$ (Tables 1 and 2).

It is clear that the substitution of Co^{2+} ions in ZnO lattice could enhance the photodegradation of the RO solution under UV light irradiation. The moderate

Table 1
Comparing the first-order photocatalytic rate constants k_A (min^{-1}) of RO dye in the presence of ZnO thin film and k_B (min^{-1}) in the presence of $Zn_{0.9}Co_{0.1}O$ at different concentration of the dyes

Dye	k_A (min^{-1})	k_B (min^{-1})	k_B/k_A
5	0.0138	0.0162	1.17
10	0.0112	0.0148	1.32
15	0.0097	0.0129	1.33
20	0.0080	0.0093	1.16

Table 2
Effect of cobalt content on the photocatalytic degradation of C.I. RO 86 textile dyes (10 ppm) in the presence of $Zn_{1-x}Co_xO$ thin film photocatalyst coated on glass

Cobalt content At%	Degradation (%)
0	50.8
1	57.4
3	61.3
5	69.3
10	78.4

concentration of cobalt in ZnO is also capable for improving the hydrogen production under solar irradiation [51]. Therefore, it is believed that the photoinduced carriers are responsible for the enhanced catalytic activity or the photodegradation of RO might proceed in a sensitized photoreaction process in combination with a catalyzed photoreaction process over $Zn_{1-x}Co_xO$ with x > 0.00, which explains the improved photocatalytic activity. The effect of initial dye concentration is attributed to the so-called shielding effect; after exceeding the optimal amount, the dye reduces the penetration of the light in the solution. Mineralization of the dyes was confirmed by monitoring the evolution of CO_2 by gas chromatography. The stoichiometry amounts of CO_2 evolved in neutral media were consistent with TOC assays. Final products were, in all cases, CO_2, NH_4^+ and NO_3^- and SO_4^{2-} ions. Results confirm the complete mineralization of the dyes.

4. Conclusion

The transparent $Zn_{1-x}Co_xO$ thin film sols have been prepared by sol–gel method with isopropanol as solvent and a novel $Zn_{1-x}Co_xO$ thin film catalyst has been prepared by dip-coating method with a flat glass as substrate. The film was characterized by means of XRD, UV-vis, SEM and AFM. It is showed that the thin film is porous, which is formed by a layer of $Zn_{1-x}Co_xO$ nano-sized particles with average diameter of 32 nm. $Zn_{1-x}Co_xO$ thin film shows stronger photoabsorption than ZnO thin film in the visible range from 450 to 800 nm. The $Zn_{1-x}Co_xO$ thin films have been employed in photocatalytic oxidation of RO. The $Zn_{1-x}Co_xO$ thin film-supported commercial glass is a promising and efficient catalyst to degrade organic pollutants. Glass coated $Zn_{1-x}Co_xO$ thin film can be used repeatedly over a long time with small loss of efficiency. This result showed that the glass coated $Zn_{1-x}Co_xO$ thin film is photochemically stable.

Acknowledgment

The authors wish to thank the Center of Excellency (Chemistry) University of Isfahan for partial financially supporting this work.

References

[1] N.M. Mahmoodi and M. Arami, Desal. Water Treat., 1 (2009) 312–317.
[2] J.L. Li, L. Liu, Y. Yu, Y.W. Tang, H.L. Li and F.P. Du, Electrochem. Commun., 6 (2004) 940–3.
[3] J. Bandara, C.C. Hadapangoda and W.G. Jayasekera, Appl. Catal., B 50 (2004) 83–8.
[4] D. Shchukin, S. Poznyak, A. Kulak and P. Pichat, J. Photochem. Photobiol., A 162 (2004) 423–30.
[5] F. Banat, S. Al-Asheh, R. Zomaout, B. Qtaishat, T. Alateat and S. Almayta, Desal. Water Treat., 5 (2009) 283–289.
[6] M. Nasr-Esfahani and M.H. Habibi, Desal. Water Treat., 3 (2009) 64–72.
[7] M.H. Habibi, A. Hassanzadeh and Mahdavi, J. Photochem. Photobiol., A 172 (2005) 89–96.
[8] M.H. Habibi, A. Hassanzadeh and A. Zeini-Isfahani, Dyes Pigm., 69 (2006) 111–117.
[9] M.H. Habibi and H. Vosoghian, J. Photochem. Photobiol., A 174 (2005) 45–52.
[10] M.H. Habibi, S. Tangestaninejad and B. Yadollahi, Apll. Catal., B 33 (2001) 57–64.
[11] T. Pauporte and J. Rathousky, J. Phys. Chem., C 111 (2007) 7639–7644.
[12] T. Yoshida, M. Iwaya, H. Ando, T. Oekermann, K. Nonomura, D. Schlettwein, D. Wohrle and H. Minoura, Chem. Commun., 4 (200) 400–404.
[13] T. Pauporte´, T. Yoshida, D. Komatsu and H. Minoura, Electrochem. Solid-State Lett., 9 (2006) H16–19.
[14] E. Michaelis, D. Wohrle, J. Rathousky and M. Wark, Thin Solid Films, 497 (2006) 163–7.
[15] T.E. Jaramillo, S.H. Baeck, A. Kleiman-Shwarsctein, E.W. McFarland, Macromol. Rapid Commun., 25 (2004) 297–9.
[16] N. M. Mahmoodi, M. Amiri and K. Gharanjig, Desal. Water Treat., 1 (2009) 312–317.
[17] S.I. Abou-Elela and M.A. El-Khateeb, Desal. Water Treat., 7 (2009) 1–5.
[18] P. Bansal, N. Bhullar and D. Sud, Desal. Water Treat., 12 (2009) 108–113.
[19] S.X. Zhou and W.G. Xu, Environ. Progress Sus. Energy, 28 (2009) 227–34.
[20] C.H. Li, F.B. Li and C.S. Li, Dyes Pigm., 76 (2008) 477–484.
[21] M. Muruganandham and M. Swaminathan, Dyes and Pigm., 68 (2006) 133–142.
[22] X.Z. Li and F.B. Li, Environ. Sci. Technol., 35 (2001) 2381–2387.
[23] J. J. Young, S. Cynthia and O. Taein, Mater. Res. Bull., 41 (2006) 67–69.
[24] C. Sampa, C. Basab, B. Sekhar, D. Paramita and K.D. Binay, J. Hazard. Mater., 154 (2008) 230–236.

[25] N. Sobana, L. Selvam and M. Swaminathan, Sep. Purific. Technol., 62 (2008) 648–653.
[26] M. P. Anna and L. Holger, Catal. Today, 137 (2008) 357–361.
[27] Qi Xiao, Jiang Zhang, Chong Xiao and Xiaoke Tan, Mater. Sci. Eng., B 142 (2007) 121–125
[28] H. Wang, C. Xie, W. Zhang, S. Cai, Z. Yang and Y. Gui, J. Hazard. Mater., 141 (2006) 645–9.
[29] A.A. Khodja, T. Sehili, J.F. Pilichowski and P. Boule, J. Photochem. Photobiol. A: Chem., 141 (2001) 231–239.
[30] D. Chatterjee and A. Mahata, Catal. Commun., 2 (2001) 1–3.
[31] C. Ye, Y. Bando, G. Shen and D. Golberg, J. Phys. Chem., B 110 (2006) 15146–15154.
[32] M.H. Habibi and M. Khaledi-Sardashti, J. Adv. Oxid. Tech., 12 (2009) 231–239.
[33] C.B. Fitzgerald, M. Venkatesan, J.G. Lunney, L.S. Dornelse and J.M.D. Coey, Appl. Surf. Sci., 247 (2005) 493–496.
[34] J.H. Kim, H. Kim, D. Kim, S.G. Yoon and W.K. Choo, Solid State Commun., 131 (2004) 677–682.
[35] S. Deka and P.A. Joy, Solid State Commun., 134 (2005) 665–669.
[36] Y.D. Kim, S.L. Cooper, M.V. Klein and B.T. Jonker, Phys. Rev., B 49 (1994) 1732–1742.
[37] X.Q. Qiu, L.P. Li and G.S. Li, Appl. Phys. Lett., 88 (2006) 114103–8.
[38] J.J. Wu, S.C. Liu and M.H. Yang, Appl. Phys. Lett., 85 (2004) 1027–32.
[39] X. Qiu, G. Li, X. Sun, L. Li and X. Fu, Nanotechnology, 19 (2008) 215703–11.
[40] C.B. Fitzgerald, M. Venkatesan, J.G. Lunney, L.S. Dorneles and J.M.D. Coey, Appl. Surf. Sci., 247 (2005) 493–496.
[41] J.H. Kim, H. Kim, D. Kim, S.G. Yoon and W.K. Choo, Solid State Commun., 131 (2004) 677–680.
[42] J.H. Kim, H. Kim, D. Kim, Y.E. Ihm and W.K. Choo, J. Appl. Phys., 92 (2002) 6066.
[43] R.A. Spurr and H. Myers, Anal. Chem., 29 (1957) 760–762.
[44] D. Chauhan, V.R. Satsangi, S. Dass and R. Shrivastav, Bull. Mater. Sci., 29 (2006) 709–715.
[45] A. Ashrafi and C. Jagdish, J. Appl. Phys., 102 (2007) 071101.
[46] A.Y. Oral, E. Mensur, M.H. Aslan and E. Basaran, Mater. Chem. Phys., 83 (2004) 140–148.
[47] D.R. Acosta, L. Castaneda, A. Lopez–Suarez and A. Guillen-Santiago, Physica, B 404 (2009) 1427–1431.
[48] Y.W. Wang, L.Z. Zhang, K.J. Deng, X.Y. Chen and Z.G. Zou, J. Phys. Chem., C 111 (2007) 2709–15
[49] X.Q. Qiu, L.P. Li, X.Z. Fu and G.S. Li, J. Nanosci. Nanotechnol., 8 (2008) 1301–8.
[50] Q. Wan, T.H. Wang and J.C. Zhao, Appl. Phys. Lett., 87 (2005) 083105.
[51] T.F. Jaramillo, S.H. Baeck, A. Kleiman-Shwarsctein, K.S. Choi, G.D. Stucky and E.W. McFarland, J. Comb. Chem., 7 (2005) 264–269.